

# Flexible Pavement Analysis Considering Temperature Profile and Anisotropy Behavior in Hot Mix Asphalt Layer

Joonho Choi<sup>1</sup>, Youngguk Seo<sup>2</sup>, Sung-Hee Kim<sup>3\*</sup>, Samuel Beadles<sup>4</sup>

<sup>1</sup>Postdoctoral Research Fellow, Georgia Institute of Technology, Atlanta, USA

<sup>2</sup>Pavement Research Group, Korea Expressway Corporation, Seongnam-si, South Korea

<sup>3</sup>Assistant Professor, Civil and Construction Engineering, Southern Polytechnic State University, Marietta, USA

<sup>4</sup>Civil and Construction Engineering, Southern Polytechnic State University, Marietta, USA

E-mail: Joonho@gatech.edu, seoyg89@hotmail.com, {\*skim4, sbeadles}@spsu.edu

Received September 20, 2011; revised October 31, 2011; accepted November 14, 2011

## Abstract

A three Dimensional finite element model (FEM) incorporating the anisotropic properties and temperature profile of hot mix asphalt (HMA) pavement was developed to predict the structural responses of HMA pavement subject to heavy loads typically encountered in the field. In this study, ABAQUS was adopted to model the stress and strain relationships within the pavement structure. The results of the model were verified using data collected from the Korean Highway Corporation Test Road (KHCTR). The results demonstrated that both the base course and surface course layers follow the anisotropic behavior and the incorporation of the temperature profile throughout the pavement has a substantial effect on the pavement response predictions that impact pavement design. The results also showed that the anisotropy level of HMA and base material can be reduced to as low as 80% and 15% as a result of repeated loading, respectively.

**Keywords:** Anisotropic Behavior, Finite Element Method, Aggregate Base, HMA

## 1. Introduction

Existing FEMs that model the behavior of layers in HMA pavement rely on simplifying assumptions about the variations of the properties within the pavement. Specifically, existing models assume linear and isotropic variations within the layers of the pavement and use the annual maximum or minimum pavement temperature to recommend a suitable asphalt binder performance grade. These assumptions are made in order to reduce the computational complexity involved in modeling the behavior of HMA pavement. A number of researchers, however, have shown that the pavement materials exhibit nonlinear, anisotropic behavior [1-4]. Researchers also mentioned that the structural or load-carrying capacity of the pavement varies with temperature for HMA layer and it is necessary to predict the temperature distribution within the HMA layers to accurately determine in situ strength characteristics of flexible pavement [5].

This paper deals with the predictions of the pavement critical responses using three dimensional FEM analysis technique. The FEM developed using ABAQUS in this study incorporates the anisotropic properties of the HMA

and base layers with temperature profile variations through the HMA layer. The approach was also validated by comparing measured pavement responses with the predictions of the three dimensional finite element analysis results.

## 2. Anisotropic Behavior of Granular Materials

Inherent anisotropy in granular materials exists even before the pavement is subjected to traffic due to the effects of compaction and gravity [6]. Stresses due to construction operations and traffic are anisotropic and new particle contacts are formed due to breakage and slippage of particles, which induces further anisotropy [6]. To more accurately investigate the effect of stress-dependency of granular materials on pavement response and surface deflection predictions, researchers developed a method to fully characterize the stress-sensitive and cross-anisotropic properties of unbound aggregate bases, which are resilient moduli in the vertical and radial directions,  $E_y$  and  $E_x$ ; shear modulus in vertical direction,  $G_{xy}$ ; Poisson's ratio for strain in the vertical direction due to a

horizontal direct stress,  $\sigma_{xy}$ ; and Poisson's ratio for strain in any horizontal direction due to a horizontal direct stress,  $\nu_{xx}$  [2,4].

As expressed in Equations (1) through (3), the modulus of the unbound aggregate base was modeled using an Uzan type stress-dependent model with a cross-anisotropic approach based on the recent studies that emphasized the importance of accounting not only for stress dependency but also the anisotropy in order to properly model the unbound aggregate modulus properties and the stress state distributions in the layer [2,4].

$$E_y = k_1 \left( \frac{I}{P_a} \right)^{k_2} \left( \frac{\tau_{oct}}{P_a} \right)^{k_3} \quad (1)$$

$$n = \frac{E_x}{E_y} \quad (2)$$

$$m = \frac{G_{xy}}{E_y} \quad (3)$$

In Equations (1), (2), and (3),  $E_y$  is the vertical modulus,  $E_x$  is the horizontal modulus,  $G_{xy}$  is the shear modulus,  $I$  is the first stress invariant (bulk stress),  $\tau_{oct}$  is the octahedral shear stress,  $P_a$  is the atmospheric pressure, and  $k_i$  are material model parameters obtained from regression analyses of the laboratory modulus test data.

To consider the anisotropic behavior of HMA layer, the horizontal and shear moduli ratio was approximated and used as an input for the FEM analysis.

### 3. Field Response Test

The KHCTR has been regarded as the most realistic research tool to evaluate the performance of pavements influenced by many complex variables such as construction, traffic, climatic, materials, etc. Test road in Korea was first constructed in December 2002 and opened to traffic in March 2004. Road research institute at the Korea Highway Corporation (KHC) played a leading role in the construction and operation of this test road, and conducted a wide range of field tests to better characterize the response and performance of highway pavements [7,8]. The KHCTR is located between the Yeo-ju junction on Interstate 50 and the Gam-gok interchange on Interstate 45, and it goes almost parallel to the Interstate

45. This two-lane, 7.7 km-long highway was composed of 25 concrete and 33 asphalt sections as illustrated in **Figure 1**.

With projected AADT (Average Annual Daily Traffic) of 57,520 in year 2011 and a load distribution factor of 0.8, the traffic volume for a 10-year design life was estimated to be 44.7 million 80-kN ESALs (Equivalent Single Axle Loads) for all pavement sections. The AASHTO interim design guide was adopted for the structural design of both pavement types. Detailed information on design and construction of the KHCTR can be found elsewhere [9].

Approximately 1900 sensors were installed at KHCTR to obtain stress and strain responses and to monitor moisture and temperature variations at different locations of sections during construction. Most of asphalt sections were instrumented with 636 sensors that include strain gauges, soil pressure cells and thermal couples. **Figure 2** illustrates a sensor layout for one of asphalt sections, A5, where strain gauges were placed in longitudinal and transverse directions to quantify the anisotropic levels in HMA layers. In **Figure 2**, ASTM 19 is the 19-mm dense graded HMA used for surface layer, BB5 is the 25-mm dense graded HMA used for intermediate layer, and BB3 is the 25-mm dense graded HMA used for base layer. Thermocouples were also embedded from the surface to the bottom of asphalt layer and those measurements were considered as inputs for the FEM described in subsequent sections.

A series of moving load tests was performed at A5 with a dump truck. A three-axle dump truck (single tire front and dual tire rear tandem) with a 12R22.5 type radial tire was utilized as a load source all along. This test vehicle was operated by the same highly trained driver to minimize natural sway in a moving vehicle. The planar configuration of tire and axle is seen in **Figure 3**. During testing, air pressures for tires of each axle were maintained at levels: 1076 kPa (1st axle), 828 kPa (2nd axle), and 1076 kPa (3rd axle). These pressure levels have been determined by averaging field survey data collected at countrywide weighing stations in Korea.

The test results conducted was selected for the implementation of FEM developed in this study. The full-scale pavement test results were shown in **Table 1**. First and second values in the table were the minimum and maximum from the experiments, respectively.

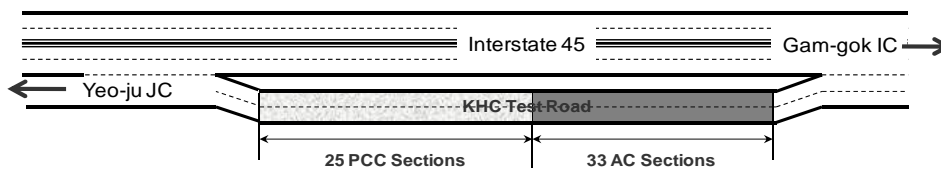


**Figure 1.** Plan view of KHCTR.

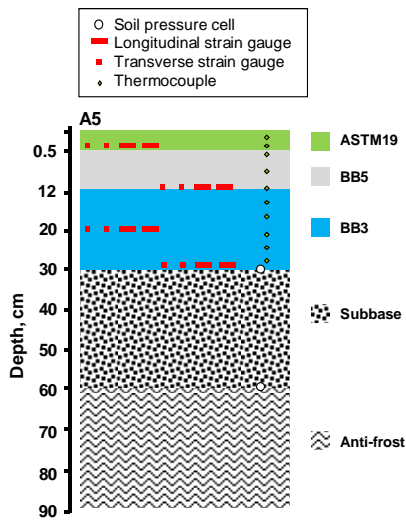


Figure 2. Cross-section and sensor layout of A5 at KHCTR.

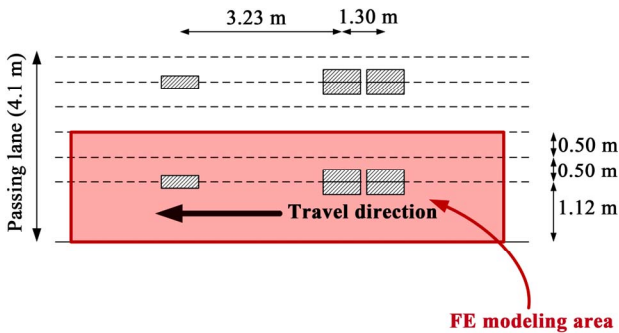


Figure 3. Plan view of the passing lane at A5 asphalt section.

Table 1. Performance response summary of pavement test sections.

Top Anti-frost		Top Subbase		Bottom AC
Vertical Stress (kPa)	Vertical Strain (10 <sup>-6</sup> )	Vertical Stress (kPa)	Vertical Strain (10 <sup>-6</sup> )	Horizontal Strain (10 <sup>-6</sup> )
19.3 - 24.8	N/A	36.4 - 81.9	N/A	30.6 - 56.5

### 4. Analysis of the Results

A pavement comprised of a 120-mm HMA layer, a 180-mm unstabilized base course, a 300-mm thick stress softening subbase layer, and a 300-mm thick anti-frost layer was used for the KHCTR section model. As shown in Figures 1 and 2, a three-axle truck was passing through the lane and the half of the area was adapted to the FE simulation. The red area shows the FEM model part and FEM model was generated. Figure 4 showed the three dimensional finite element mesh model representing loading area and the red area on the top represented the loading location. The perimeter boundary conditions were assumed as simply supported. Loads of

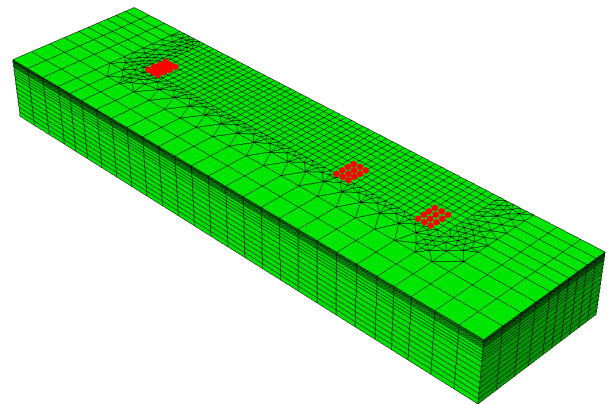


Figure 4. Finite Element (FE) model with mesh and loading area.

27.2 kN, 21.5 kN, and 21.9 kN were applied for front, middle, and back tire areas respectively. A fixed boundary condition was also assumed at the bottom of the section. A regression equation that fits the temperature profile data was developed as shown in Equation (4) and implemented into the FEM model.

$$\text{Temperature} = 20.411(\text{depth})^{-0.175} \quad (4)$$

In order to develop values for vertical and horizontal resilient modulus ratios, twelve sensitive analyses were performed with different level of anisotropy. All materials were assumed as anisotropic material except anti-frost layer and Table 2 shows the material properties used in the FEM models.

Table 3 shows the comparisons between the measured data collected from the KHCTR and FEM results for the simulations. Based on comparisons, the higher value of the vertical strain at the top of anti-frost layer was obtained when the unbound aggregate base and HMA layer were modeled as 15% level of anisotropy and 70% level of anisotropy. Similarly, the tensile strains at the bottom transitioned from the linear isotropic case without considering the temperature profile variation to the anisotropic analyses with the consideration of temperature profile variation throughout the HMA layer. These are the critical pavement responses that are directly related to rutting and asphalt fatigue cracking that significantly contribute to the overall pavement performance and overlay design.

Table 3 also compares the measured pavement responses with the three dimensional FEM predictions from the different analyses. In general, the predicted pavement responses from FEM analysis with the anisotropic model for HMA and aggregate base are in reasonably good agreement with the measured pavement responses from KHCTR when the HMA layer and Base layer is considered as 80% and 15% level of anisotropy, separately,

**Table 2. Anisotropic material properties.**

Simulation Number	Layer Type	Thickness (m)	Vertical Resilient Modulus (MPa)	Vertical Poisson's Ratio	Horizontal Resilient Modulus (MPa)	Horizontal Poisson's Ratio	Shear Stress (MPa)
HMA: 70% Base: 15%	HMA	0.12	2760	0.35	1930	0.245	1930
	Base	0.18	517	0.35	78	0.05	78
	Subbase	0.30	241	0.35	36	0.05	36
	Anti-frost	0.30	69	0.40	-	-	-
HMA: 70% Base: 30%	HMA	0.12	2760	0.35	1930	0.245	1930
	Base	0.18	517	0.35	155	0.11	155
	Subbase	0.30	241	0.35	72	0.11	72
	Anti-frost	0.30	69	0.40	-	-	-
HMA: 70% Base: 50%	HMA	0.12	2760	0.35	1930	0.245	1930
	Base	0.18	517	0.35	259	0.18	259
	Subbase	0.30	241	0.35	121	0.18	121
	Anti-frost	0.30	69	0.40	-	-	-
HMA: 80% Base: 15%	HMA	0.12	2760	0.35	2210	0.28	2210
	Base	0.18	517	0.35	78	0.05	78
	Subbase	0.30	241	0.35	36	0.05	36
	Anti-frost	0.30	69	0.40	-	-	-
HMA: 80% Base: 30%	HMA	0.12	2760	0.35	2210	0.28	2210
	Base	0.18	517	0.35	155	0.11	155
	Subbase	0.30	241	0.35	72	0.11	72
	Anti-frost	0.30	69	0.40	-	-	-
HMA: 80% Base: 50%	HMA	0.12	2760	0.35	2210	0.28	2210
	Base	0.18	517	0.35	259	0.18	259
	Subbase	0.30	241	0.35	121	0.18	121
	Anti-frost	0.30	69	0.40	-	-	-
HMA: 90% Base: 15%	HMA	0.12	2760	0.35	2480	0.32	2480
	Base	0.18	517	0.35	78	0.05	78
	Subbase	0.30	241	0.35	36	0.05	36
	Anti-frost	0.30	69	0.40	-	-	-
HMA: 90% Base: 30%	HMA	0.12	2760	0.35	2480	0.32	2480
	Base	0.18	517	0.35	155	0.11	155
	Subbase	0.30	241	0.35	72	0.11	72
	Anti-frost	0.30	69	0.40	-	-	-
HMA: 80% Base: 50%	HMA	0.12	2760	0.35	2480	0.32	2480
	Base	0.18	517	0.35	259	0.18	259
	Subbase	0.30	241	0.35	121	0.18	121
	Anti-frost	0.30	69	0.40	-	-	-

**Table 3. FEM results with different anisotropic level.**

Anisotropy Level	Top Anti-frost		Bottom Subbase		Top Subbase		Bottom Base		Top Base		Bottom AC
	Vertical Stress (kPa)	Vertical Strain ( $10^{-6}$ )	Vertical Stress (kPa)	Vertical Strain ( $10^{-6}$ )	Vertical Stress (kPa)	Vertical Strain ( $10^{-6}$ )	Vertical Stress (kPa)	Vertical Strain ( $10^{-6}$ )	Vertical Stress (kPa)	Vertical Strain ( $10^{-6}$ )	Horizontal Strain ( $10^{-6}$ )
HMA: 70% Base: 15%	23.5	300	26.5	120	40.2	180	46.8	100	68.5	140	59
HMA: 70% Base: 30%	17.8	240	20.4	100	36.9	166	45.9	109	76.6	155	36
HMA: 70% Base: 50%	14.2	190	16.1	95	33.4	154	44.0	110	81.5	159	19
HMA: 80% Base: 15%	<b>22.8</b>	<b>285</b>	<b>25.6</b>	<b>116</b>	<b>38.3</b>	<b>168</b>	<b>44.4</b>	<b>98</b>	<b>64.3</b>	<b>132</b>	<b>54</b>
HMA: 80% Base: 30%	17.4	230	19.8	102	35.4	159	43.8	104	72.3	147	34
HMA: 80% Base: 50%	13.9	185	15.8	92	32.2	148	42.1	106	77.3	152	18
HMA: 90% Base: 15%	22.1	276	24.8	112	36.7	160	42.3	93	60.7	125	50
HMA: 90% Base: 30%	17.1	225	19.4	99	34.1	153	42.0	100	68.6	140	32
HMA: 90% Base: 50%	13.7	181	15.5	90	31.1	144	40.5	102	73.7	146	18
Isotropic, (Temperature Variation Not Considered)	21.8	272	24.4	111	35.9	157	41.4	92	59.3	122	90
Exp	19.3 -24.8				36.4 -81.9						30.6 -56.5

with the temperature profile consideration throughout the pavement. This indirectly shows that anisotropic modeling and temperature variation consideration of HMA and base layers provide a much more realistic approximation of the measured responses. With better and more accurate predictions of these responses, a more structurally adequate pavement can be designed.

## 5. Conclusions

The synergistic effect of anisotropic behavior of HMA and base layers considering the temperature variation throughout the HMA layer was investigated by performing a three dimensional finite element analyses. The results from the ABAQUS finite element models clearly showed that anisotropic model of both the asphalt and aggregate base layers gave the most realistic predictions when compared to measured values for pavement responses. Substantially higher critical pavement responses were predicted with the increased anisotropic level of HMA and base layer. Horizontal strain is a critical pavement response, which is directly related to fatigue

performance, and the level of anisotropy of HMA and aggregate base impacts the stress and strain distributions. With better and more accurate predictions of these responses, a structurally more adequate pavement can be designed.

## 6. References

- [1] S. H. Kim, D. N. Little and E. Tutumluer, "Validated Model for Predicting Field Performance of Aggregate Base Courses," *Transportation Research Record* 1873, 2003.
- [2] S. H. Kim, D. N. Little and E. Masad, "Simple Methods to Estimate Inherent and Stress-Induced Anisotropic Level of Aggregate Base," *Transportation Research Record* 1913, TRB, National Research Council, Washington DC, 2005, pp. 24-31.
- [3] S. H. Kim, D. N. Little and E. Tutumluer, "Effect of Gradation on Nonlinear Stress-Dependent Behavior of a Sandy Flexible Pavement Subgrade," *Journal of Transportation Engineering*, Vol. 133, No. 10, 2007, pp. 582-589. [doi:10.1061/\(ASCE\)0733-947X\(2007\)133:10\(582\)](https://doi.org/10.1061/(ASCE)0733-947X(2007)133:10(582))
- [4] E. Tutumluer, D. N. Little and S. H. Kim, "Validated

- Model for Predicting Field Performance of Aggregate Base Courses,” *Transportation Research Record* 1837, TRB, National Research Council, Washington DC, 2003, pp. 41-49.
- [5] B. K. Diefenderfer, I. L. Al-Qadi and S. D. Diefenderfer, “Model to Predict Pavement Temperature Profile: Development and Validation,” *Journal of Transportation Engineering*, Vol. 132, No. 2, 2006, pp. 162-167. [doi:10.1061/\(ASCE\)0733-947X\(2006\)132:2\(162\)](https://doi.org/10.1061/(ASCE)0733-947X(2006)132:2(162))
- [6] J. J. Dong and Y. W. Pan, “Micromechanics Model for Elastic Stiffness of Non-Spherical Granular Assembly,” *International Journal for Numerical and Analytical Methods in Geomechanics*, Vol. 23, 1999, pp. 1075-1100. [doi:10.1002/\(SICI\)1096-9853\(199909\)23:11<1075::AID-NAG24>3.0.CO;2-S](https://doi.org/10.1002/(SICI)1096-9853(199909)23:11<1075::AID-NAG24>3.0.CO;2-S)
- [7] Y. Seo, “Distress Evolution in Highway Flexible Pavements: A 5-Year Study at the KHC Test Road,” *ASTM Journal of Testing and Evaluation*, Vol. 38, No. 1, 2010, pp. 32-41.
- [8] Y. Seo, “A Full Scale in Situ Evaluation of Strain Characteristics at Highway Flexible Pavement Sections,” *ASTM Journal of Testing and Evaluation*, Vol. 38, No. 4, 2010, pp. 390-399.
- [9] Korea Highway Corporation, “A Study on the Construction and Management of Korea Highway Test Road,” *Final Report*, 2002.